Theoretical and Experimental Studies of the Diketene System: Product Branching Decomposition Rate Constants and Energetics of Isomers

BINH BUI,[1] TI JO TSAY,[2] M. C. LIN,[2] C. F. MELIUS[3]

[1]*University of Georgia, Athens*, GA 30602-2556
[2]*Emory University, Atlanta*, GA 30322-2210
[3]*Lawrence Livermore National Laboratory, Livermore*, CA 94551

Received 18 September 2006; revised 5 March 2007; accepted 6 March 2007

DOI 10.1002/kin.20263
Published online in Wiley InterScience (www.interscience.wiley.com).

ABSTRACT: The kinetics and mechanism for the thermal decomposition of diketene have been studied in the temperature range 510–603 K using highly diluted mixtures with Ar as a diluent. The concentrations of diketene, ketene, and CO_2 were measured by FTIR spectrometry using calibrated standard mixtures. Two reaction channels were identified. The rate constants for the formation of ketene (k_1) and CO_2 (k_2) have been determined and compared with the values predicted by the Rice–Ramsperger–Kassel–Marcus (RRKM) theory for the branching reaction. The first-order rate constants, k_1 (s^{-1}) $= 10^{15.74 \pm 0.72}$ exp(-49.29 (kcal mol^{-1}) (± 1.84)/RT) and k_2 (s^{-1}) $= 10^{14.65 \pm 0.87}$ exp(-49.01 (kcal mol^{-1}) (± 2.22)/RT); the bulk of experimental data agree well with predicted results. The heats of formation of ketene, diketene, cyclobuta-1,3-dione, and cyclobuta-1,2-dione at 298 K computed from the G2M scheme are -11.1, -45.3, -43.6, and -40.3 kcal mol^{-1}, respectively. © 2007 Wiley Periodicals, Inc. Int J Chem Kinet 39: 580–590, 2007

Correspondence to: M. C. Lin: e-mail: chemmcl@emory.edu. National Science Council Distinguished Visiting Professor at Chiao-tung University, Hsinchu, Taiwan.

Contract grant sponsor: Basic Energy Sciences, U. S. Department of Energy.
Contract grant number: DE-FG02-97-ER14784.

INTRODUCTION

The gas phase thermal decomposition of diketene under diluted conditions has been known to efficiently produceketene [1].

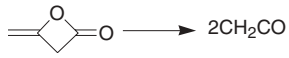

(1)

Experiments with kinetic isotope effect studies were performed by Chikos to establish that the thermolysis equation (1) is first order [2]. Furthermore, the activation energy of the concerted reaction has been determined to be 50 kcal mol^{-1} [3]. The pyrolysis of diketene can also occur through another reaction pathway to give allene and carbon dioxide [4,5].

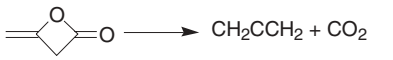

(2)

Calculations made by Rice and Roberts using the standard state heats of formation of ketene, allene, and carbon dioxide suggested that this channel was more likely to occur thermodynamically than (1) [6]. Secondary reactions that may occur under high-conversion conditions include ketene reacting to form cyclobuta-1,3-dione

(3)

or 2, 4-dimethylene-1,3-dioxetane

(4)

In principle, these isomers of diketene, cyclobuta-1,3-dione, and 2,4-dimethylene-1,3-dioxetane may also be formed by the direct isomerization of diketene and may subsequently fragment into two ketene molecules, i.e., the reverse of (1), (3), and (4).

Although there have been no comprehensive kinetic studies on diketene pyrolysis, a few groups have published theoretical results that are directly related to our study and should be mentioned here as a prelude to our investigation. Jug et al. [7] calculated the activation energies for the fragmentation of three isomeric species to form ketene as well as their corresponding reverse reactions by using the semiempirical SINDO method. The reverse reaction paths of (3) and (4) were estimated to have energy barrier of approximately the same height. Their results also concluded that the isomerization of diketene to form cyclobutane-1,3-dione and 2,4-dimethylene-1,3-dioxetane could not occur due to energy barrier considerations and the likelihood of fragmentation at higher energies. Fu et al. [8] studied the dimerization reactions of ketene and obtained a very high activation energy of 61.2 kcal mol^{-1} by MP2/4-31G for the 2,4-dimethylene-1,3-dioxetane forming pathway (4). Seidl and Schaefer [9] determined by CISD+Q/DZ+P that the 2,4-dimethylene-1,3-dioxetane molecule was energetically less stable than diketene by 32 kcal mol^{-1}, compared with the value of 42 kcal mol^{-1} computed by Fu. Although these theoretical studies provide us a qualitative idea of the reaction scheme involved in diketene pyrolysis, they are quantitatively in discordance.

Diketene as well as its monomer, ketene, is commercially important. Despite the claim made by Rice and Roberts [6] that reaction (2) could occur, no attempt has been made to give a theoretical interpretation of this channel. The aim of our work is, therefore, to experimentally measure the rate constants for the branching dissociation of diketene by reactions (1) and (2) and to compare these values with those predicted by the transition state theory (TST) or the Rice–Ramsperger–Kassel–Marcus (RRKM) theory for examination of pressure effect, based on the computational results of various methods including G2M (modified Gaussian-2) [10] and BAC-G3B3 [11]. By comparing experiment to theory, we are testing the accuracy of our results and of the theoretical model.

Our interest in diketene arises in part from the fact that it is isoelectronic with the dimer of HNCO. In an earlier study on the thermal reaction of isocyanic acid between 900 and 1200 K, a new bimolecular process

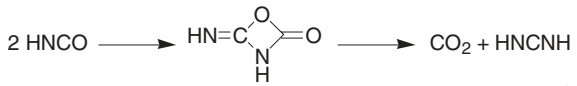

(5)

was proposed to account for the production of CO_2 and nitrogen-containing products, such as HCN and NH_3 [12]. Employing the same mechanism and similar transition state geometries as in (5), we can conveniently explain (1) and (2).

EXPERIMENTAL SECTION

The thermal decomposition of diketene was carried out in a 270-mL quartz reactor cell heated with a double-walled cylindrical furnace. A thermocouple placed in a sealed tube at the center of the cell was used to measure and maintain the temperature, monitored by an Omega CN-9000 solid-state temperature controller. Prior to each run, the entire system, i.e. the cell, the vacuum line, and the FTIR sample cell, was pumped down to 10^{-4} Torr. The chamber enclosing the sample cell was purged with dry N_2 gas in order to remove water, carbon dioxide, and other impurities that could potentially mar the spectrum. After the pyrolysis, the reaction mixture was analyzed with a Mattson Instrument Polaris FT-IR spectrometer.

The pyrolysis of diketene was studied in the temperature range 510–603 K, corresponding to reacting

times of a few minutes to several hours. Most of the runs were carried out at a constant pressure of 800 Torr with high Ar-dilution in order to minimize any reactions occurring on the surface of the reaction cell and to prevent air leakage into the system. However, several runs were performed between 100 and 800 Torr with 100-Torr increments in order to test the pressure dependence of the rate constants. Three different concentrations of diketene, highly diluted with ultra pure argon, were included in our study: 0.14%, 0.26%, and 0.52%.

The products measured and calibrated by FTIR analysis were diketene, ketene, and carbon dioxide at 1012.6, 2163.0, and 2361.7 cm^{-1}, respectively. Figure 1 shows a typical set of spectra for a pyrolyzed (B and C band signal) and unpyrolyzed (A band signal) sample of a diketene mixture. The CO_2 and diketene used in this work were initially obtained from Aldrich with purities of 99.8% and 98%, respectively. Diketene was further purified by trap-to-trap distillation from 273 to 195 K (dry ice temperature). The purified sample was a clear and colorless liquid. The result of FTIR analysis revealed no detectable impurities such as CO_2, CH_2CO, and CH_3COOH. Ketene was prepared by the pyrolysis of acetic anhydride (Aldrich) at around 773 K. The main product, ketene, was then repeatedly distilled from 195 to 148 K (*n*-propanol slush bath) to eliminate CO_2 impurities.

Experimental Data

The decomposition of the 0.14%, 0.26/%, and 0.52% diketene–argon mixtures was measured in the temperature range 510–603 K while maintaining a constant pressure 800 Torr as alluded to above. The calibration allowed us to convert the measured reactant and product absorbance into concentration versus time profiles for each of the temperature studied. These profiles were kinetically modeled by using the following equations with the initial concentration of diketene, $[DK]_0$:

$$[DK]_t = [DK]_0 \exp[-(k_1 + k_2)t] \quad (6)$$

$$[CH_2CO]_t = [(2k_1[DK]_0)/(k_1 + k_2)]\{1 - \exp[-(k_1 + k_2)t]\} \quad (7)$$

$$[CO_2]_t = [(k_2[DK]_0)/(k_1 + k_2)]\{1 - \exp[-(k_1 + k_2)t]\} \quad (8)$$

Consequently, the total rate constants ($k_{tot} = k_1 + k_2$) can in principle be derived from the above equations through fitting the diketene, ketene, or CO_2 concentration profiles. Evaluation of Eqs. (7) and (8) can yield the values of k_1 and k_2, respectively. k_1 can be directly derived from ketene yields or indirectly from the difference k_{tot} (by [diketene]) $-k_2$ (by $[CO_2]$). The results from both methods are in reasonable agreement as shown in Fig. 2a. In Fig. 2b, we compare the values of total rate constant derived from the decay of diketene with $k_1 + k_2$ obtained from the analyses using ketene and CO_2 concentration profiles, respectively. Table I lists the experimental rate constants for the two channels in the temperature range 510–603 K for comparison with the computed values (vide infra). The rate constants were fitted with the standard form of the Arrhenius equation by weighted least-squares method to yield the following expressions for k_1 and k_2:

$$k_1\ (s^{-1}) = 10^{15.74 \pm 0.72}\ \exp(-49.29(\text{kcal mol}^{-1})(\pm 1.84)/RT) \quad (9)$$

$$k_2\ (s^{-1}) = 10^{14.65 \pm 0.87}\ \exp(-49.01(\text{kcal mol}^{-1})(\pm 2.22)/RT) \quad (10)$$

where $R = 1.987 \times 10^{-3}$ kcal mol^{-1} K^{-1}.

The values of k_1 and k_2 were then inserted in Eqs. (7) and (8) to remodel the concentration profiles of ketene and CO_2. Figure 3 illustrates examples of concentration profiles of this system along with the corresponding modeling results. In general, the agreement between experimental and computed profiles is good, except those of ketene at higher temperatures and longer reaction times, probably due to the loss by polymerization.

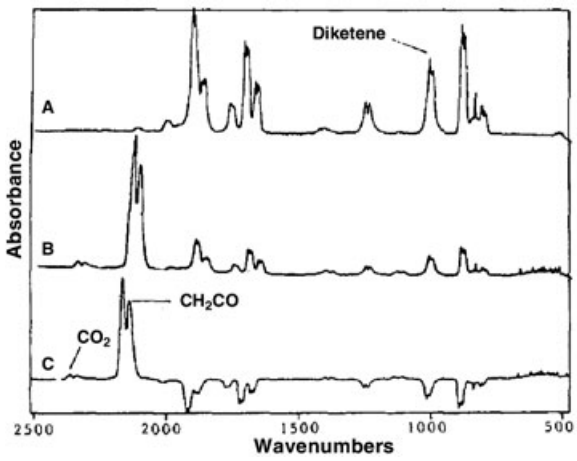

Figure 1 (A) 319.0 Torr of 0.26% diketene in Ar, unpyrolyzed. (B) 0.26% diketene in Ar pyrolyzed at 801.9 Torr and 573 K for 21 h and 48 min. The final pressure after expansion was 319.0 Torr. (C) The difference between A and B.

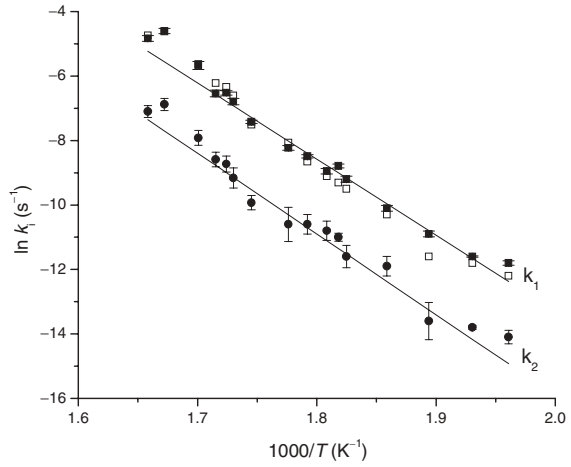

(a)

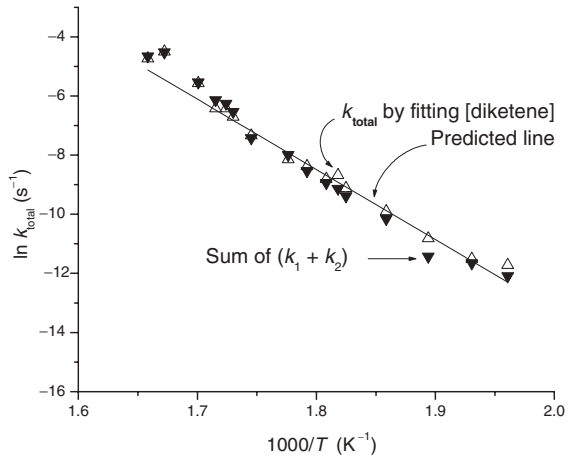

(b)

Figure 2 The experimentally modeled rate constants: (a) k_1 (■) resulted from [k_{tot} (of DK fitting) – k_2], k_1 obtained from direct fitting of [ketene] (□), and k_2 (●) from fitting [CO_2]; predicted values are shown in solid lines; (b) total rate constants: k_{tot} resulted from [DK] fitting (▼), and sum of [k_1 + k_2] (Δ), respectively obtained from direct fitting of [ketene] and [CO_2]; predicted values are shown in solid lines.

Computational

We employed the hybrid density functional method [13], B3LYP, with the 6-311G (d,p) basis set for geometric optimization of the reactant, transition structures (TSs), and products. The intrinsic reaction coordinate (IRC) [14,15] calculations were utilized to confirm the nature of respective TSs. Thermal and zero-point vibrational corrections of all species were obtained at the same level of theory through the calculation of the harmonic analytic vibrational frequencies.

Higher level single point calculations were also carried out with the optimized geometries using the modified Gaussian-2 (G2M) [10] method to improve the predicted energies. We applied the G2M(RCC5) scheme to calculate the base energy (E_{base}) at the MP4/6-311G(d,p) level of theory and improve the E_{base} with an expanded basis set correction ($\Delta E(+3df2p)$), a restricted couple cluster ($\Delta E(RCC)$) correction, and the "higher level correction" (HLC) based on the number of paired (n_α) and unpaired (n_β) valence electrons. The following is a summary of the G2M scheme:

$$E_{base} = E[PMP4/6\text{-}311G(d,p)] \quad (11)$$

$$\Delta E(RCC) = E[RCCSD(T)/6\text{-}311G(d,p)] - E_{base} \quad (12)$$

$$\Delta E(+3df2p) = E[MP2/6\text{-}311 + G(3df, 2p)] - E[MP2/6\text{-}311G(d,p)] \quad (13)$$

$$\Delta E(HLC, RCC5) = -5.25n_\beta - 0.19n_\alpha \quad (14)$$

$$E[G2M(RCC5)] = E_{base} + \Delta E(RCC) + \Delta E(+3df2p) + \Delta E(HLC, RCC5) + ZPE \quad (15)$$

All calculations were performed using the Gaussian-98 program [16]. Optimized geometries along with bonding information are provided in Fig. 4. Energetic parameters, ZPE, moments of inertia, and frequencies, together with high-level relative energies obtained from the G2M scheme are tabulated and used in our discussion (vide infra). Also, we compare the energetic data with those obtained by the bond additivity correction (BAC-G3B3) [11] procedure. Table II includes relative energies of diketene and its cyclic isomers; Table III contains relative energies of species resulted from the diketene reaction; Table IV provides molecular and TS parameters needed for the standard RRKM calculation implemented in the ChemRate program [17].

RESULTS AND DISCUSSION

Diketene and Its Cyclic Isomers

In Fig. 4, the geometries of diketene and its cyclic isomers, 1,3-cyclobutadione and 2,4-dimethylene-1,3-dioxetane, are presented together with two other geometric isomers, 1,2-cyclobutadione and 3,4-dimethylene-1,2-dioxetane. The structure of diketene is compared with available experimental data reported by Bregman and Bauer [18]. The predicted C—C and C—O bond distances agree with those from the electron diffraction study within 0.01 Å, well within the experimental uncertainty of ±0.04 Å.

Table I Experimental and Predicted Rate Constants, k_1 and k_2, versus Temperature at 800 Torr

	Experimental		Predicted	
Temperature (K)	k_1	k_2	k_1	k_2
510	7.36E–06	7.81E–07	4.11E–06	3.19E–07
518	8.93E–06	1.07E–06	8.38E–06	6.79E–07
528	1.87E–05	1.28E–06	1.98E–05	1.69E–06
538	4.31E–05	6.87E–06	4.51E–05	4.07E–06
548	1.01E–04	9.17E–06	10.00E–05	9.47E–06
553	1.30E–04	2.01E–05	1.47E–04	1.43E–05
558	2.06E–04	2.44E–05	2.15E–04	2.14E–05
563	2.66E–04	2.41E–05	3.13E–04	3.18E–05
573	6.01E–04	4.87E–05	6.46E–04	6.86E–05
578	1.13E–03	1.05E–04	9.20E–04	9.97E–05
583	1.44E–03	1.86E–04	1.30E–03	1.44E–04
588	3.46E–03	3.62E–04	1.83E–03	2.07E–04
598	1.01E–02	1.03E–03	3.56E–03	4.18E–04
603	8.02E–03	8.26E–04	4.92E–03	5.89E–04

Molecular structures of 1,3-cyclobutanedione (D_{2h}) and 2,4-dimethylene-1,3-dioxetane (D_{2h}) fit within 0.02 Å or less, to those predicted by Seidl and Schaeffer [9] using the DZ+P SCF level of theory. The C—O distances are 1.386 Å in 2,4-dimethylene-1,3-dioxetane, and the other bond lengths, C—C, are 1.544 Å in 1,3-cyclobutanedione, respectively. Obviously, the ring strain effect in 1,3-dioxetane may account for the 27.5 kcal mol^{-1} higher in energy than 1,3-cyclobutanedione.

The other two isomers of diketene are 3,4-dimethylene-1,2-dioxetane and 1,2-cyclobutanedione. They have a higher symmetry order, belonging to the C_{2v} symmetry point group, than diketene (C_s). They are not directly derivable from diketene through isomerization. 1,2-Cyclobutanedione is only 3.3 kcal mol^{-1} energetically higher than 1,3-cyclobutanedione or 4.7 kcal mol^{-1} above diketene; however, it was not mentioned in any recent experiments or theoretical calculations. While 2,4-dimethylene-1,3-dioxetane lies 29.0 kcal mol^{-1} above diketene as compared to the values of 32 and 42 kcal mol^{-1}, respectively, reported by Schaefer and Fu; our BAC-G3B3 value [11] of 29.4 is the closest to the G2M value. 3,4-Dimethylene-1,2-dioxetane is located at 84.0 kcal mol^{-1} relative to diketene on the potential energy surface (PES).

At each level of theory except for one, diketene isomer is predicted to be the lowest on the potential energy surface (Table II). At MP4(SDTQ) level of theory, 1,3-cyclobutanedione isomer is 0.7 kcal mol^{-1} more stable than diketene; this was predicted as well in Seidl and Schaeffer's calculations, i.e., 0.7 kcal mol^{-1} (CISD) and 0.8 kcal mol^{-1} (Davidson-corrected CISD) [9]. However, our final G2M and BAC-G3B3 values indicate that 1,3-cyclobutanedione lies above diketene by 1.5 and 2.2 kcal mol^{-1}, respectively.

Mechanism of Diketene Decomposition

Both reactions (1) and (2) occur through concerted mechanisms. In (1), the decomposition of diketene to form two ketene fragments occurs with the elongation of C(4)—O(7) bond in the TS1 from 1.397 to 2.323 Å accompanied by the rotation of one ketene moiety at −50.8° with respect to the other one, and the extension of the C(1)—O(6) bond from 1.508 to 1.697 Å. Vibrational frequency analyses and IRC tests were performed on TS1 to confirm its geometric transformation and to validate the concerted nature of the transition structure.

Diketene decomposition in reaction (2) occurs through TS2 to form allene and carbon dioxide. The breaking C(6)—O(7) and C(1)—C(4) bonds in TS2 are 2.105 and 1.806 Å, respectively; the TS preserves the C_s symmetry point group of the reactant. The concerted nature of this reaction path is similar to TS1 and has been confirmed by an IRC test.

Figure 5 displays the PES of diketene decomposition computed at the G2M and BAC-G3B3 levels. At the G2M level of theory, the barrier of (1), 45.1 kcal mol^{-1}, is 3.0 kcal mol^{-1} lower than that of reaction (2) (48.1 kcal mol^{-1}). The BAC-G3B3 method predicts a similar trend as the G2M method, i.e., 45.5 and 47.8 kcal mol^{-1} for TS1 and TS2, respectively. Although in our rate constant calculation, we employed the values predicted by the G2M method (whose applicability has been widely demonstrated in our previous studies [19–25]), the BAC-G3B3 method should give essentially the same results.

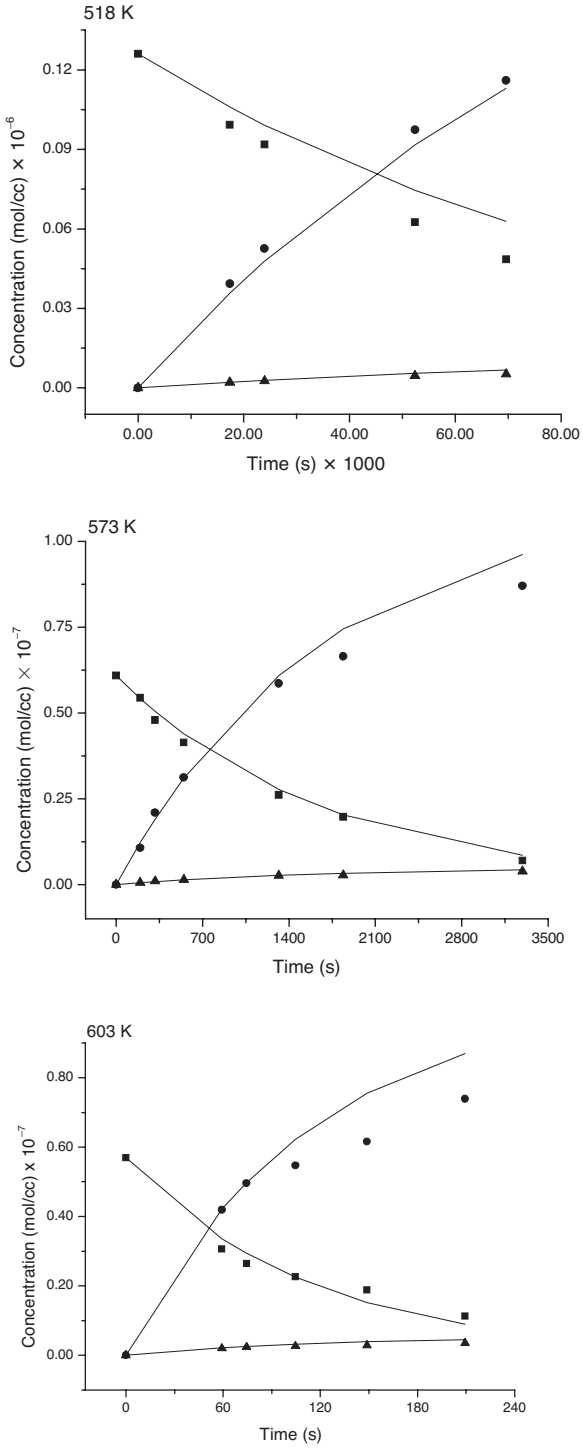

Figure 3 Concentration versus time plotted for diketene (■), ketene (●), and CO_2 (▲), at (a) 518 K (800 Torr), (b) 573 K (800 Torr), and (c) 603 K (800 Torr); modeling values using the experimentally fitted k_1 and k_2 are expressed in solid lines.

In addition, the PES displays other two high-lying channels leading to the 4-methyl-oxet-2-one intermediate that could be concertedly fragmented into methylacetylene and CO_2 through TS5. However, these pathways are not possible due to high barriers of the TS3 and TS4 (75.3 and 101.7 kcal mol^{-1}, respectively). Both TS3 and TS4 describe the hydrogen transfer from the cyclic methylene moiety to the external methylene unit. While in TS3, the leaving hydrogen atom is directly positioned at a dihedral angle of -49.6° with respect to the molecular plane, in TS4 the corresponding hydrogen atom is located at -0.84°. The TS4 barrier is higher in energy because its transformation involves the reconfiguration of the π-electrons in the C=C bond, i.e., elongation from 1.319 to 1.396 Å, and the rotation of the external methylene unit. Also, in principle the dimerization of two ketenes can occur through TS6, 44.9 kcal mol^{-1}, to form 1,3-cyclobutadione, which is located 1.5 kcal mol^{-1} above diketene. However, Tenud et al. [26] reported that there was only a small trace amount of 1,3-cyclobutadione produced from dimerization of ketenes that leads mainly to diketene. The reaction of two ketenes to yield 2,4-dimethylene-1,3-dioxetane is unlikely because of the high barrier of TS7 (52.1 kcal mol^{-1}) and the low stability of the product (29.0 kcal mol^{-1} above diketene).

Rate Constant Calculations

The rate constants for the unimolecular decomposition of diketene were calculated at temperatures between 510 and 1000 K by using ChemRate [17]. Argon was considered as bath gas according to experimental conditions. The exponential-down equation [27,28] with a step size of $\langle \Delta E \rangle_{\text{down}} = 350$ cm^{-1} was applied to model the collisional energy transfer using appropriate Lennard–Jones (L–J) parameters for the Ar-adduct collision pairs, i.e. Ar [29] ($\sigma = 3.47$ Å, $\varepsilon = 113.5$ K) and diketene ($\sigma = 3.95$ Å, $\varepsilon = 173.0$ K). The L–J parameters of diketene were deconvoluted from the DK–He complex collision parameters (σ_{cplx}, $\varepsilon_{\text{cplx}}$) [27–29] obtained from a direct fit of the computed Lennard–Jones potential curve of the complex using the equation

$$V_{\text{L-J}} = 4\varepsilon_{\text{cplx}}\left[(\sigma_{\text{cplx}}/r)^{12} - (\sigma_{\text{cplx}}/r)^{6}\right] \qquad (16)$$

where r is the center-of-mass separation between the two particles. Although the diketene's Lennard–Jones parameters are roughly approximated, their effect is negligible due to the fact that the decomposition reaction of interest was measured primarily at 800 Torr at

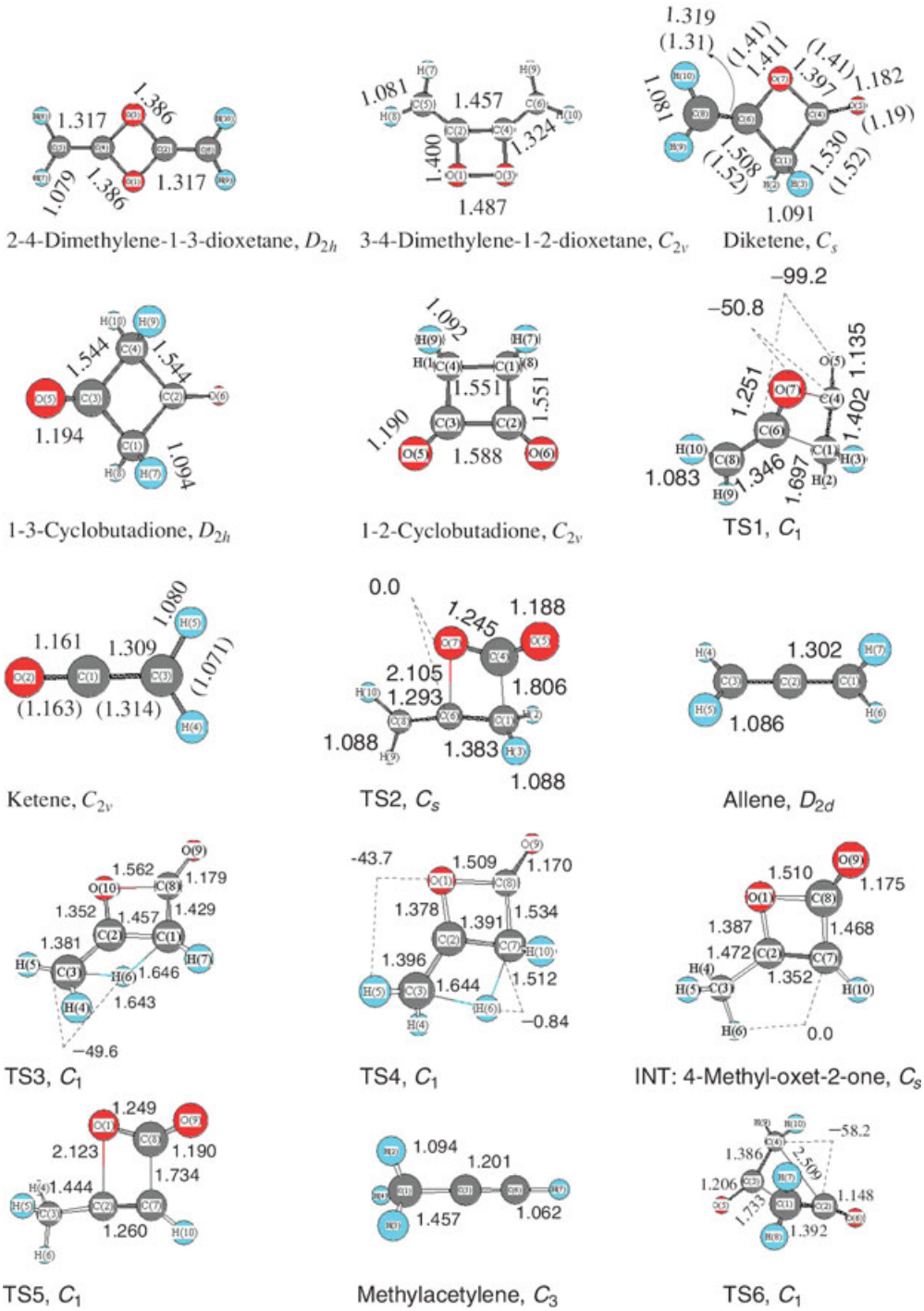

Figure 4 Optimized [B3LYP/6-311G(d,p)] molecular geometries of all studied species. [Color figure can be viewed in the online issue, which is available at www.interscience.wiley.com.]

which the rates are pressure independent. Other appropriate molecular and thermochemical parameters predicted by the G2M (Table III) were employed for the rate constant calculations. Hindered-rotor treatments were applied to the cases of TS1 and TS2, whose torsional frequencies are below 100 cm^{-1}. Predicted rate constants are fitted to the Arrhenius equation; the corresponding expressions are shown in Fig. 2.

Figure 2a displays the rate constants, k_1 and k_2 (solid lines), evaluated at 800 Torr. At different

Table II Relative Energies of Ketene's Dimers (kcal mol^{-1})

Diketene and Its Isomeric Dimers	ZPE (Unscaled)	B3LYP with ZPE	(P)MP4 (SDTQ)/ 6-311G(d,p)	RCCSD(T)/ 6-311G(d,p)	MP2/ 6-311G(d,p)	MP2/ 6-311+G(3df,2p)	G2M(RCC5) with ZPE	BAC-G3B3 with ZPE
Diketene	45.39	0.00	0.00	0.00	0.00	0.00	0.00	0.00
(2x) Ketene	39.63	10.77	20.96	23.47	22.25	25.92	21.39	22.38
2,4-Dimethylene-1,3-dioxetane	44.70	28.01	33.37	31.53	33.20	31.31	28.95	29.43
3,4-Dimethylene-1,2-dioxetane	44.04	82.44	89.76	87.49	93.28	91.18	84.04	n/a
1,2-Cyclobutadione	44.78	3.99	0.33	1.84	1.65	5.15	4.73	n/a
1,3-Cyclobutadione	44.18	0.65	−0.72	0.01	0.14	2.78	1.45	2.19

conditions of temperatures for the decomposition of diketene, reaction (1) is more favorable than reaction (2) producing allene and CO_2 as indicated by the low barrier of TS1 (45.1 kcal mol^{-1}) relatively to that of TS2 (48.1 kcal mol^{-1}). At the high-pressure and temperature limit, k_2 is likely to compete with k_1 as shown in Table V that displays the branching ratios of channel 1 (k_1/k_{tot}) and 2 (k_2/k_{tot}). Nevertheless, the branching ratio of k_1 decreases to as low as 0.73, and that of k_2 increases to as high as 0.27 at 1000 K.

At 800 Torr, the predicted results are compared with experimental values of k_1 and k_2 expressed in Fig. 2a along with the k_{tot} values displayed in Fig. 2b. The results agree well in the temperature range 510–603 K. Treatment of the hindered-rotor in TS1 and TS2 was taken into account in

Table III Molecular and Transition-State Parameters Used in the RRKM Calculation

Reaction Species	E_{rel}[a] (kcal/mol)	Symmetry Number	Moments of Inertia (10^{-40} g cm^2)	Vibrational Frequencies[b] (cm^{-1})
Diketene	0.00	1	68.78, 302.14, 365.57	136, 319, 460, 514, 530, 678, 735, 816, 864, 895, 984, 988, 1019, 1118, 1209, 1265, 1417, 1444, 1766, 1964, 3077, 3128, 3164, 3255
TS_1	45.1	1	115.65, 305.78, 344.76	460i, 92, 206, 346, 421, 484, 494, 626, 671, 711, 865, 954, 1010, 1047, 1090, 1189, 1423, 1449, 1749, 2236, 3047, 3150, 3160, 3258
Ketene	21.4	2	2.94, 81.34, 84.29	447, 563, 596, 991, 1172, 1408, 2234, 3179, 3271
TS_2	48.1	1	88.39, 312.51, 395.30	850i, 57, 245, 359, 368, 436, 479, 616, 674, 862, 870, 902, 971, 1011, 1077, 1240, 1375, 1446, 1898, 1947, 3095, 3123, 3170, 3241
Allene		4	5.75, 93.83, 93.83	372, 372, 867, 867, 885, 1017, 1017, 1109, 1423, 1480, 2052, 3117, 3122, 3192, 3192
CO_2		2	0.00, 71.53, 71.53	666, 666, 1375, 2436
TS_6	44.9	1	126.00, 313.57, 348.21	389i, 109, 207, 322, 437, 482, 548, 599, 653, 710, 805, 966, 998, 1037, 1067, 1165, 1408, 1483, 1841, 2167, 3090, 3147, 3178, 3237
1,3-Cyclobutadione	1.5	4	75.92, 321.13, 386.50	72, 374, 402, 425, 475, 537, 626, 717, 871, 917, 923, 1043, 1156, 1160, 1171, 1193, 1380, 1396, 1847, 1930, 3045, 3050, 3096, 3098

[a] Energies relative to the reactants are given at the G2M level based on the B3LYP/6-311G(d,p)geometries for the species of the system.
[b] The vibrational frequencies were computed at the B3LYP/6-311G(d,p) level of theory.

Table IV Relative Energies of Diketene, Reaction Species, and Respective Transition Structures (kcal mol^{-1})

Reaction Species	ZPE (Unscaled)	B3LYP/ 6-311G(d,p)	B3LYP[a] with ZPE	(P)MP4(SDTQ)/ 6-311G(d,p)	RCCSD(T)/ 6-311G(d,p)	MP2/ 6-311G(d,p)	MP2/ 6-311+G(3df,2p)	G2M(RCC5) with ZPE	BAC-G3B3 with ZPE
Diketene	45.39	0.00	0.00	0.00	0.00	0.00	0.00	0.00	0.00
TS1	42.43	44.92	41.96	44.75	48.75	45.59	44.94	45.15	45.46
Ketene (2x)	39.63	16.52	10.77	20.96	23.47	22.25	25.92	21.39	22.38
TS2	42.12	45.06	41.80	50.83	52.59	54.31	53.08	48.09	47.84
$CH_2CCH_2 + CO_2$	41.78	−7.84	−11.45	−5.76	−4.60	−5.13	−1.48	−4.55	−3.63
TS3	41.10	76.71	72.42	79.69	81.67	78.40	76.30	75.28	74.96
TS4	40.29	106.40	101.31	106.32	107.59	106.71	105.92	101.71	n/a
4-Methyl-oxet-2-one	44.46	7.70	6.78	6.95	7.63	6.59	6.63	6.74	7.15
TS5	42.22	45.43	42.26	49.75	51.22	53.85	52.99	47.20	46.96
$CH_3CCH + CO_2$	42.17	−6.32	−9.54	−8.94	−6.49	−10.61	−6.09	−5.18	−4.63
TS6	42.40	41.62	38.63	41.72	47.21	42.88	43.58	44.91	44.65
1,3-Cyclobutadione	44.18	1.86	0.65	−0.72	0.01	0.14	2.78	1.45	2.19

[a] B3LYP/6-311G(d,p).

the rate constant calculations to fit the experimental values.

Enthalpy of Formation of Ketene

Several existing experimental values for the heat of formation of ketene ($\Delta_f H^o_{298}$) are -11.4 ± 0.4 [30], -12.91 ± 1.20 [31], -11.85 ± 0.21 [32], and -12.8 ± 0.1 kcal mol^{-1} [33]. The first and third values, reported by Nuttal et al. [30] and Ruscic et al. [32], agree quite well within the experimental uncertainty. The fourth value, most recently reported by Traeger [33] using the photoionization mass spectrometry method, is close to the second value derived by Aubry et al. [31]. To the controversial experimental values that seem to be divided into two groups of values, many computed [34–38] $\Delta_f H^o_{298}$ of ketene support either one or the other of the two groups. We derived the new $\Delta_f H^o_{298}$ for ketene at the G2M-level by using the following heat of the reaction ($\Delta_r H^o_{298} = 50.0$ kcal mol^{-1}):

$$CO_2 + {}^3CH_2 \Leftrightarrow CH_2CO + {}^3O \qquad (17)$$

The experimental $\Delta_f H^o_{298}$ of CO_2, and ^3O are well established [39]. There are three recently reported $\Delta_f H^o_{298}$ values of $^3CH_2$, 92.60 ± 0.50, 92.90 ± 0.14, and 92.35 ± 1.00 kcal mol^{-1}, by Zabarnick et al. [40], Doltsinis and Knowles [41], and Chase [39], respectively; these values result in the following three $\Delta_f H^o_{298}$ values of ketene: -11.1, -10.8, and -11.3 kcal mol^{-1}. All three values appear to favor the higher heats of formation of Nuttall et al. [30] and Ruscic et al. [32], -11.4 ± 0.4 and -11.85 ± 0.21 kcal mol^{-1}, respectively.

Enthalpy of Formation of Diketene and Its Isomers

We employed the predicted $\Delta_f H^o_{298}$ value of ketene, -11.1 kcal mol^{-1}, and heat of reaction (1) (298 K) to obtain the $\Delta_f H^o_{298}$ value of diketene, -45.3 kcal mol^{-1}, which agrees with the experimental value, -45.47 ± 0.13 kcal mol^{-1} [42]. By using the heat of reaction between diketene and its isomers together with the predicted $\Delta_f H^o_{298}$ value of diketene, -45.3 kcal mol^{-1}, we computed the $\Delta_f H^o_{298}$ values for cyclobuta-1,3-dione, cyclobuta-1,2-dione, 2,4-dimethylene-1,3-dioxetane, and 3,4-dimethylene-1,2-dioxetane, i.e., -43.6, -40.3, -16.3, and 39.0 kcal mol^{-1}, respectively. If the experimental $\Delta_f H^o_{298}$ diketene value of –45.47 kcal mol^{-1} instead of -45.3 kcal mol^{-1}is used, the corresponding results are only 0.2 kcal mol^{-1} higher.

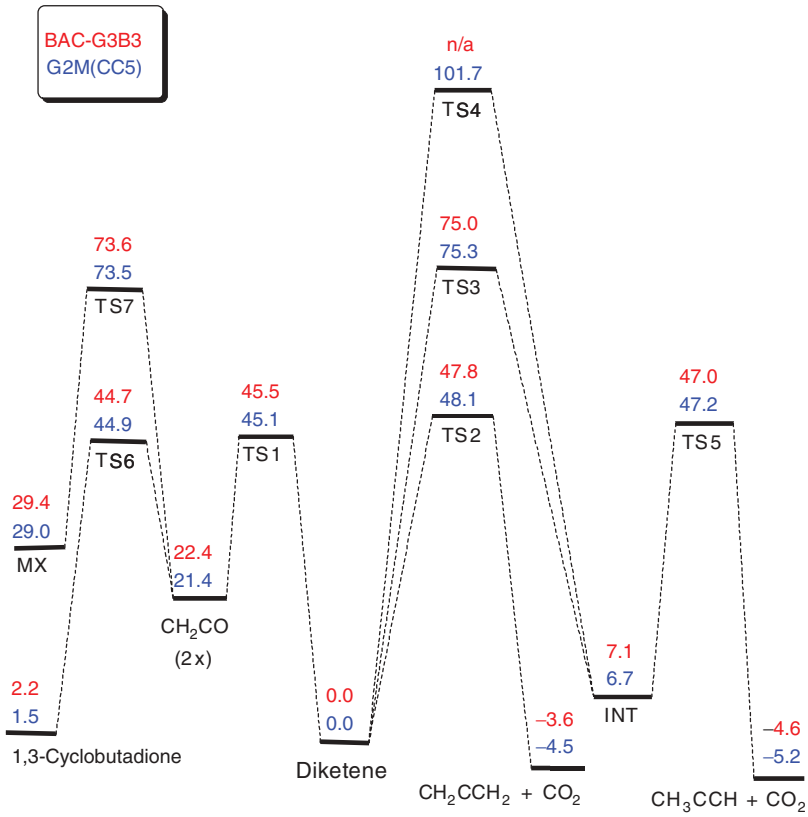

Figure 5 Potential energy surface (kcal mol^{-1}) of diketene decomposition; G2M's and BAC-G3B3's values are in boldface and normal. [Color figure can be viewed in the online issue, which is available at www.interscience.wiley.com.]

Table V Predicted Branching Ratio of k_1 and k_2 at Different Temperature and Pressure conditions

	Branching Ratio					
	Lower-Pressure Limit		760 Torr		Infinite Pressure	
Temperature	k_1	k_2	k_1	k_2	k_1	k_2
510	0.989	0.011	0.928	0.072	0.928	0.072
550	0.988	0.012	0.913	0.087	0.911	0.089
553	0.987	0.013	0.912	0.088	0.909	0.091
580	0.987	0.013	0.902	0.098	0.898	0.102
603	0.986	0.014	0.893	0.107	0.888	0.112
800	0.982	0.018	0.840	0.160	0.804	0.196
1000	0.980	0.020	0.812	0.188	0.734	0.266

CONCLUSION

The thermal decomposition of diketene has been studied experimentally in the temperature range 510–603 K by means of FTIR product analysis. The experiments were performed at 800 Torr using highly diluted Ar mixtures. The reaction was observed to be weakly pressure dependent at pressures at 100 Torr. The first-order rate constants, k_1 (s^{-1}) $= 10^{15.74 \pm 0.72}$ exp(−49.29 (kcal mol^{-1}) (±1.84)/*RT*) and k_2 (s^{-1}) $= 10^{14.65 \pm 0.87}$ exp(−49.01 (kcal mol^{-1}) (±2.22)/*RT*), the bulk of the data agrees well with those predicted at 800 Torr Ar by the quantum mechanical and statistical calculations. The fact that reaction (1) is favored is consistent with the predicted lower barrier for ketene production. The $\Delta_f H^o_{298}$ values of ketene, diketene, cyclobuta-1,3-dione, and cyclobuta-1,2-dione computed from the G2M computational scheme were −11.1, −45.3, −43.6, and −40.3 kcal mol^{-1}, respectively. Our predicted results validate the experimental data and further prove the capability of the G2M level of theory.

M. C. Lin acknowledges the support from the National Science Council of Taiwan for a Distinguished Visiting Professorship at National Chiao Tung University in Hsichu, Taiwan.

BIBLIOGRAPHY

1. Andreades, S.; Carlson, H. D. Org Synth 1965, 45, 50–54.
2. Chickos, J. S. J Org Chem 1976, 41, 3176–3179.
3. Chickos, J. S.; Sherwood, D. E., Jr. ; Jug, K. J Org Chem 1978, 43, 1146–1150.
4. Fitzpatrick, J. T. J Am Chem Soc 1947, 69, 2236.
5. Conley, R. T.; Rutledge, T. F. (Air Reduction Co., Inc.): Murray Hill, NJ, 1957.
6. Rice, F. O.; Roberts, R. J Am Chem Soc 1943, 65, 1677.
7. Jug, K.; Dwivedi, C. P. D.; Chickos, J. S. Theor Chim Acta 1978, 49, 249–257.
8. Fu, X. Y.; Fang, D.; Ding, Y. J Mol Struct 1988, 44, 349–358.
9. Seidl, E. T.; Schaefer, H. F., III. J Am Chem Soc 1990, 112, 1493–1499.
10. Mebel, A. M.; Morokuma, K.; Lin, M. C. J Chem Phys 1995, 103, 7414–7421.
11. Bharthwaj, A.; Melius, C. F. J Phys Chem A 2005, 109, 1734–1747.
12. He, Y.; Liu, X.; Lin, M. C.; Melius, C. F. Int J Chem Kinet 1991, 23, 1129–1149.
13. Becke, A. D. J Chem Phys 1993, 98, 5648–5652.
14. Gonzalez, C.; Schlegel, H. B. J Chem Phys 1990, 94, 5523–5527.
15. Gonzalez, C.; Schlegel, H. B. J Chem Phys 1989, 90, 2154–2161.
16. Frisch, M. J.; Trucks, G. W.; Schlegel, H. B.; Gill, P. M. W.; Johnson, B. G.; Robb, M. A.; Cheeseman, J. R.; Keith, T.; Petersson, G. A.; Montgomery, J. A.; Raghavachari, K.; Al-Laham, M. A.; Zakrzewski, V. G.; Ortiz, J. V.; Foresman, J. B.; Cioslowski, J.; Stefanov, B. B.; Nanayakkara, A.; Challacombe, M.; Peng, C. Y.; Ayala, P. Y.; Chen, W.; Wong, M. W.; Andres, J. L.; Replogle, E. S.; Gomperts, R.; Martin, R. L.; Fox, D. J.; Binkley, J. S.; Defrees, D. J.; Baker, J.; Stewart, J. P.; Head-Gordon, M.; Gonzalez, C.; Pople, J. A.; Gaussian, Inc.: Pittsburgh, PA, 1998.
17. Mokrushin, V.; Bedanov, V.; Tsang, W.; Zachariah, M.; Knyazev, V. National Institute of Standard and Technology: Gaithersburg, MD, 2003.
18. Bregman, J.; Bauer, S. H. J Am Chem Soc 1955, 77, 1955–1965.
19. Choi, Y. M.; Park, J.; Wang, L.; Lin, M. C. ChemPhysChem 2004, 5, 1231–1234.
20. Choi, Y. M.; Park, J.; Lin, M. C. ChemPhysChem 2004, 5, 661–668.
21. Xu, Z. F.; Park, J.; Lin, M. C. J Chem Phys 2004, 120, 6593–6599.
22. Zhu, R. S.; Xu, Z. F.; Lin, M. C. J Chem Phys 2004, 120, 6566–6573.
23. Xu, Z. F.; Lin, M. C. Int J Chem Kinet 2004, 36, 205–215.
24. Xu, Z. F.; Lin, M. C. Int J Chem Kinet 2004, 36, 178–187.
25. Tokmakov, I. V.; Moskaleva, L. V.; Lin, M. C. Int J Chem Kinet 2004, 36, 139–151.
26. Tenud, L.; Weilenmann, M.; Dallwigk, E. Helv Chim Acta 1977, 60, 975–977.
27. Gilbert, R. G.; Smith, S. C. Theory of Unimolecular and Recombination Reactions; Blackwell: Oxford, UK, 1990.
28. Tardy, D. C.; Rabinovitch, B. S. J Chem Phys 1966, 45, 3720–3730.
29. Mourits, F. M.; Rummens, F. H. A. Can J Chem 1977, 55, 3007–3020.
30. Nuttall, R. L.; Laufer, A. H.; Kilday, M. V. J Chem Thermodyn 1971, 3, 167–174.
31. Aubry, C.; Holmes, J. L.; Terlouw, J. K. J Phys Chem A 1997, 101, 5958–5961.
32. Ruscic, B.; Litorja, M.; Asher, R. L. J Phys Chem A 1999, 103, 8625–8633.
33. Traeger, J. C. Int J Mass Spectrom 2000, 194, 261–267.
34. Scott, A. P.; Radom, L. Int J Mass Spectrom Ion Processes 1997, 160, 73–81.
35. Nguyen, M. T.; Nguyen, H. M. T. Chem Phys Lett 1999, 300, 346–350.
36. Curtiss, L. A.; Raghavachari, K.; Redfern, P. C.; Pople, J. A. J Chem Phys 1997, 106, 1063–1079.
37. Curtiss, L. A.; Raghavachari, K.; Redfern, P. C.; Rassolov, V.; Pople, J. A. J Chem Phys 1998, 109, 7764–7776.
38. Sumathi, R.; Green, W. H., Jr. J Phys Chem A 2002, 106, 7937–7949.
39. Chase, M. W. NIST-JANAF Thermochemical Tables, J Phys Chem Ref Data, no. 9; A.C.S.: Washington, DC, 1998.
40. Zabarnick, S.; Fleming, J. W.; Lin, M. C. J Chem Phys 1986, 85, 4373–4376.
41. Doltsinis, N. L.; Knowles, P. J. J Chem Soc, Faraday Trans 1997, 93, 2025–2027.
42. Mansson, M.; Nakase, Y.; Sunner, S. Acta Chem Scand 1968, 22, 171–174.